Surface Science 605 (2011) 539–544

Contents lists available at ScienceDirect

Surface Science

journal homepage: www.elsevier.com/ locate/susc

Interface effects in the electronic structure of TiO_2 deposited on MgO, Al_2O_3 and SiO_2 substrates

L. Soriano [a,*], M. Sánchez-Agudo [b], R.J.O. Mossanek [c], M. Abbate [c], G.G. Fuentes [d], P.R. Bressler [e,1], L. Alvarez [f], J. Méndez [f], A. Gutiérrez [a], J.M. Sanz [a]

[a] Departamento de Física Aplicada, Instituto de Ciencia de Materiales Nicolás Cabrera, Universidad Autónoma de Madrid, Cantoblanco, 28049 Madrid, Spain
[b] ITM CIDA, Arturo Soria 289, E-28033 Madrid, Spain
[c] Departamento de Física, Universidade Federal do Paraná, Caixa Postal 19044, 81531-990 Curitiba PR, Brazil
[d] Centro de Ingeniería Avanzada de Superficies, AIN. 31191 Cordovilla-Pamplona, Spain
[e] Helmholtz Zentrum Berlin für Materialien und Energie, Elektronenspeicherring BESSY II, Albert-Einstein-Str. 15, 12489 Berlin, Germany
[f] Instituto de Ciencia de Materiales de Madrid, CSIC, Cantoblanco, E-28049 Madrid, Spain

ARTICLE INFO

Article history:
Received 20 September 2010
Accepted 13 December 2010
Available online 21 December 2010

Keywords:
Synchrotron radiation photoelectron spectroscopy
X-ray absorption spectroscopy
Interface states
Titanium oxide
Silicon oxide
Aluminum oxide
Magnesium oxide

ABSTRACT

We report the Ti 2p X-ray absorption (XAS) and resonant photoemission (RPES) spectra of one equivalent TiO_2 monolayer grown on MgO, Al_2O_3 and SiO_2 substrates. The Ti 2p XAS spectra of these systems were compared to atomic multiplet calculations projected in different octahedral crystal fields. The comparison indicates that the crystal field splitting and the Ti–O hybridization decrease along the MgO, Al_2O_3 and SiO_2 series. The analysis of the RPES spectra provides the Ti 3d contributions to the valence band in these systems. These were compared to configuration interaction calculations of a TiO_6 cluster for different Ti 3d–O 2p hybridizations. The Ti 3d states in the valence band shift to lower binding energies along the MgO, Al_2O_3 and SiO_2 series. These effects are attributed to changes in the electronic structure at the interface, which, in turn, are related to the formation of cross-linking Ti–O–M (M = Mg, Al, and Si) bonds.

1. Introduction

Thin oxide films present unique electrical, optical, magnetic and chemical properties. Thus, they are increasingly used as a coating elements in many technological applications, for example, optoelectronic devices, gas sensors and supported catalysis. But the properties of these films are strongly related to the growth conditions. In particular, they depend on the interaction with the corresponding substrate. For this reason, the study of these interfaces is attracting considerable attention. Many of these studies are focused on the electronic structure, because this determines the microscopic origin of their physical properties.

There are several studies on the electronic structure of oxide surfaces produced in the early nineties [1–4]. Since then, many works that focused on oxide/oxide interfaces using different characterization techniques have been performed [5]. The analysis of oxide/oxide interfaces has been always a difficult task due to different effects, such as substrate preparation and orientation, the thickness and morphology of the thin film, etc. To this end, new empirical tools like the "chemical state vector" were proposed to study oxide/oxide interfaces [6]. In many cases, the influence of the substrate can lead to the formation of mixed oxides at the interface, whose electronic structure and physical properties differ from those of the corresponding single oxides. The importance of these novel materials in technological applications can be found in several review works in the field of catalysis [7], spintronic [8], sensors [9] and microelectronics [10].

The study of TiO_2/SiO_2 ultra-thin films found an increase of the band gap for very low coverages [11], where the authors pointed out that the nature of the substrate was more important than the layer thickness. The interface was characterized by photoemission spectroscopy (PES) and extended X-ray absorption fine structure (EXAFS), suggesting the formation of distinct Si–O–Ti cross-linking bonds at the interface [12]. These results indicated a strong interfacial interaction between both oxides, and the need for a further characterization using other techniques. Further, a variation of the Auger parameter of TiO_2 thin films grown on alumina and silica substrates was attributed to interface effects [13]. Other related works show that TiO_2 can be epitaxially grown on α-Al_2O_3 single crystal [14,15] as well as on MgO (100) single crystal [16].

X-ray absorption spectroscopy (XAS) is, in a first approximation, a technique related to the unoccupied electronic states [17]. XAS was applied to the study of bulk compounds, such as oxides, nitrides and

* Corresponding author. Tel.: +34 913974192; fax: +34 913973969.
E-mail address: l.soriano@uam.es (L. Soriano).
[1] Fraunhofer-Gesellschaft, Brussels Unit 31, Rue du Commerce, 1000 Brussels, Belgium.

0039-6028/$ – see front matter © 2010 Elsevier B.V. All rights reserved.
doi:10.1016/j.susc.2010.12.013

carbides [18]. The work by Himpsel et al. [19] showed that XAS could be used to study surfaces and buried interfaces. Since then, several works presented XAS spectra of different oxide surfaces and oxide/oxide interfaces [20–22]. On the other hand, resonant photoemission (RPES) was widely used to study the electronic structure of bulk compounds. This technique is used to obtain the metal contribution to the valence band in covalent compounds [23]. Bourgeois et al. noted that the crystalline structure may affect the high energy part of the TiO_2 valence band spectra [24]. The electronic structure of TiO_2 was studied using RPES at 3p [25,26] and at 2p edges [27–29]. As already observed in other works, the resonance effects are stronger at the 2p edge [27,30].

It is important to note that the oxide substrates used here were polycrystalline or even amorphous, and had a very different morphology (see below). In spite of that, we show that XAS and RPES do provide information on interface effects for coverages below the monolayer regime. Indeed, we already showed that TiO_2/oxide interface effects are mainly observed for coverages up to one equivalent monolayer, independently from the growth conditions of the TiO_2 thin film and the morphology of the substrate [20,29].

The substrates were prepared as thin films using different conventional methods on conductive supports, thus avoiding experimental charging artifacts during the photoemission measurements. This is of extreme importance when using intense synchrotron radiation to obtain PES spectra. To explore the influence of the substrate we used MgO, Al_2O_3 and SiO_2, which present differences in the covalent-ionic contribution to the bonding at the interface. Important interface effects have already been observed in the Ni 2p PES spectra of NiO thin films deposited on the same set of substrates [31].

In this work, we study the electronic structure of TiO_2 deposits of approximately one equivalent monolayer (1 ML) grown on MgO, Al_2O_3 and SiO_2. The experimental techniques were X-ray absorption spectroscopy (XAS) and resonant photoemission (RPES). The XAS spectra were compared to atomic multiplet calculations, whereas the RPES spectra were compared to cluster model calculations. The trends observed in these systems are related to the relative ionic character of the substrate, due to the formation of cross-linking Ti–O–M (M = Mg, Al, and Si) bonds at the interfaces.

2. Experimental details

The corresponding oxide substrates were prepared *in situ* on conductive materials following conventional methods. More details on the preparation and characterization procedures can be found elsewhere [31]. The TiO_2 thin films were grown on the different oxide substrates by reactive thermal evaporation of Ti. The substrates were held at room temperature and the partial pressure of oxygen was about 2.0×10^{-5} mbar (base pressure = 10^{-9} mbar). The TiO_2 deposits were grown *in situ* in successive steps in a preparation chamber attached to the analysis chamber. After each step, they were analyzed with the corresponding technique. The thickness of the thin films was controlled by quantitative analysis of the PES and XAS intensities [20]. The spectra analyzed here correspond to approximately one equivalent TiO_2 monolayer (1 ML), where interface effects are clearly observable (see below). The spectra of the thin films were compared with an anodic TiO_2 sample used as a reference.

The XAS measurements were performed at the VLS-PGM beamline located at the BESSY II storage ring [32]. The estimated resolution of the XAS spectra is better than 100 meV at the Ti 2p edge (about 450 eV). The spectra were collected using the total electron yield method (a −10 V bias voltage was applied to reduce the background of secondary electrons). The energy scale was calibrated using the known peak positions of the Ti 2p Electron-Energy-Loss (EELS) spectrum [33]. The spectra were normalized to the I_0 current measured in a gold sample. The RPES measurements were performed at the SU8 beamline of the SuperAco storage ring of LURE. This beamline was equipped with an undulator and a plane grating-spherical mirror monochromator. The valence band photoemission spectra were measured with an angle resolved electron analyzer from VSW. The valence band spectra were measured using photon energies throughout the Ti 2p → 3d absorption edge (455–471 eV). The spectra were normalized to the I_0 current measured using a gold mesh. The overall (monochromator plus analyzer) energy resolution at these energies was better than 100 meV. Atomic force microscopy (AFM) images were measured in dynamic mode (tapping) using a Nanotec's microscope and software [34].

3. Calculation details

The electronic structure of TiO_2 was calculated using a cluster model solved by configuration interaction. The cluster consisted of a $[TiO_6]^{-8}$ octahedron structure resulting in a Ti^{4+} ion with a nominal $3d^0$ occupancy. The ground state was expanded in the $3d^0$, $3d^1\underline{L}$, $3d^2\underline{L}^2$, $3d^3\underline{L}^3$, etc. configurations, where $\underline{L}$ denotes a hole in the O 2p band. The final states were obtained by either removing (valence band) or adding (conduction band) an electron. The corresponding spectral weight $A(\omega)$ in each case was calculated using the sudden approximation. The Ti 2p XAS spectra were calculated with an atomic multiplet program, which considers the $3d^0$ and $3d^1\underline{L}$ configurations and include crystal field effects [35].

The main parameters of the model are the charge-transfer energy Δ, the Mott–Hubbard repulsion U and the p–d transfer integral (pdσ). The multiplet splitting was obtained in terms of the crystal field parameters 10 Dq, as well as the p–p transfer integral (ppπ)–(ppσ). The calculations were performed in octahedral symmetry, where the Ti 3d levels are split into the Ti t_{2g} and Ti e_g states. The intra-atomic exchange parameter J was ignored because the TiO_2 compound is non-magnetic. The values of the model parameters used in the calculation of TiO_2 are listed in Table 1. These values gave the best agreement with the experiment and are similar to previous estimates [35].

4. Results and discussion

4.1. Morphological characterization of the substrates

The morphology of the different oxide substrates has been characterized by AFM. Fig. 1 shows the $1\times1\ \mu m^2$ images of the SiO_2, Al_2O_3, and MgO substrates. The AFM images show that the morphology of the substrates is significantly different. The roughness varies two orders of magnitude, from 0.3 nm for SiO_2, to 4.5 nm for Al_2O_3, and 73.4 nm for MgO. This is not surprising if one takes into account the preparation method for each substrate: SiO_2 is the result of the thermal oxidation of a Si wafer; Al_2O_3 was obtained by thermal oxidation of a polycrystalline Al foil, and MgO has been obtained by reactive evaporation of Mg at room temperature. More details on the preparation of the substrates were already published elsewhere [31]. For a small TiO_2 coverage we expect that the results would be strongly affected by interface effects, whereas for a large TiO_2 coverage we would expect to recover the bulk behavior.

Table 1
Cluster model parameters (all values in eV).

	TiO_2	TiO_2/MgO	TiO_2/Al_2O_3	TiO_2/SiO_2
Δ	4.0	4.0	4.0	4.0
U	4.5	4.5	4.5	4.5
pdσ	2.1	1.9	1.7	1.5
10 Dq	1.8	1.6	1.4	1.2
ppσ	0.9	0.9	0.9	0.9
	0.0	0.0	0.0	0.0

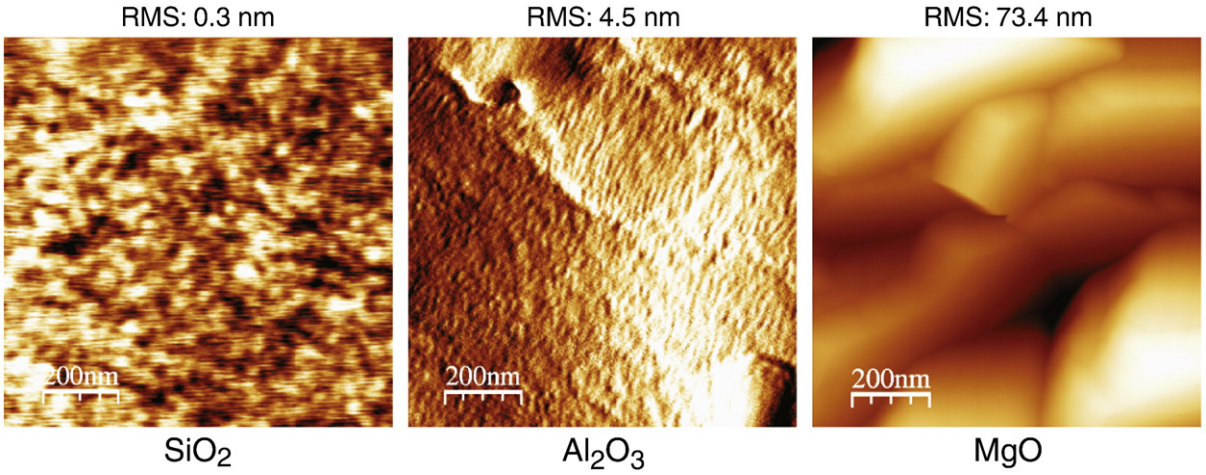

Fig. 1. $1 \times 1\ \mu m^2$ AFM images of the different oxide surfaces measured in dynamic mode (tapping). The rms roughness values are given for comparison.

4.2. Ti 2p XAS spectra

The O 1s XAS spectra would provide direct information on the unoccupied Ti 3d states of the TiO_2 thin films [36]. But the stronger signal coming from the oxygen atoms of the oxide substrates hides this information. On the other hand, the Ti 2p XAS spectra provide site and symmetry selected information, which is not hindered by the electronic states of the substrate. These XAS spectra can be explained as an atomic multiplet projected in the corresponding crystal field [37]. Fig. 2 shows the experimental XAS spectra of the TiO_2 films grown on the different substrates as a function of the coverage. They are formed by four main peaks (labeled as A, B, C and D). In a first approximation, the peaks A and B come from transitions from Ti $2p_{3/2}$ states, whereas the peaks C and D correspond to transitions from Ti $2p_{1/2}$ states. On the other hand, peaks A (C) and B (D) are assigned to transitions to Ti t_{2g} and Ti e_g states respectively [37]. The spectra corresponding to high coverages are similar and resemble those of bulk TiO_2. For coverages below one equivalent monolayer, the spectra clearly differ from those for large coverages. This indicates that up to one equivalent monolayer the spectra are dominated by interface effects. Finally, the results for intermediate coverages can be reproduced by a linear combination of the interface and the bulk TiO_2 spectra.

To understand the experimental spectra for low coverages, we have performed multiplet calculations for a Ti^{4+} ion projected in octahedral symmetry. Fig. 3 shows the calculated Ti 2p XAS spectra for the different values of the crystal field parameter 10 Dq. The black dashed line corresponds to the first ionic approximation ($3d^0$), whereas the red solid line includes the hybridization with the ligand states ($3d^1\underline{L}$). These results show that these spectra are highly sensitive to both the crystal field and covalence effects.

Fig. 4 shows the experimental Ti 2p XAS spectra of the TiO_2 reference sample, as well as those corresponding to one equivalent TiO_2 monolayer grown on MgO, Al_2O_3 and SiO_2. The spectra of the reference sample shows the same basic structures reported in the literature for TiO_2 [33]. As stated before, the peaks at 458.0 and 459.6 eV correspond mostly to transitions from the Ti $2p_{3/2}$ to Ti t_{2g}

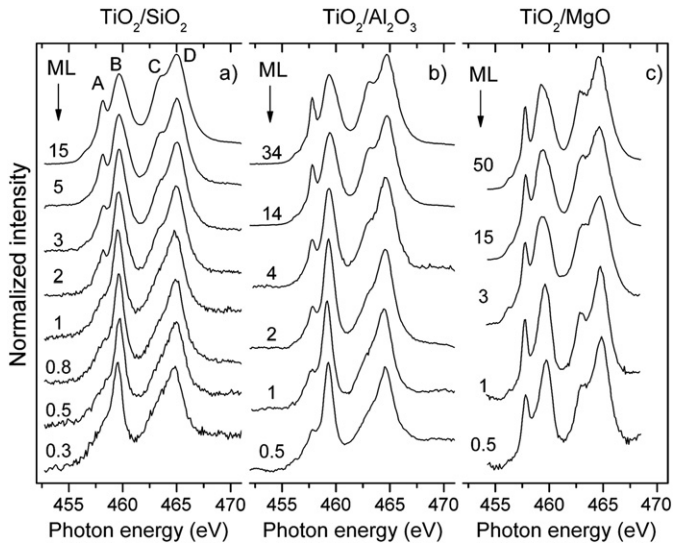

Fig. 2. The Ti 2p XAS spectra of the TiO_2 thin films grown on the different oxide substrate as a function of the coverage in ML.

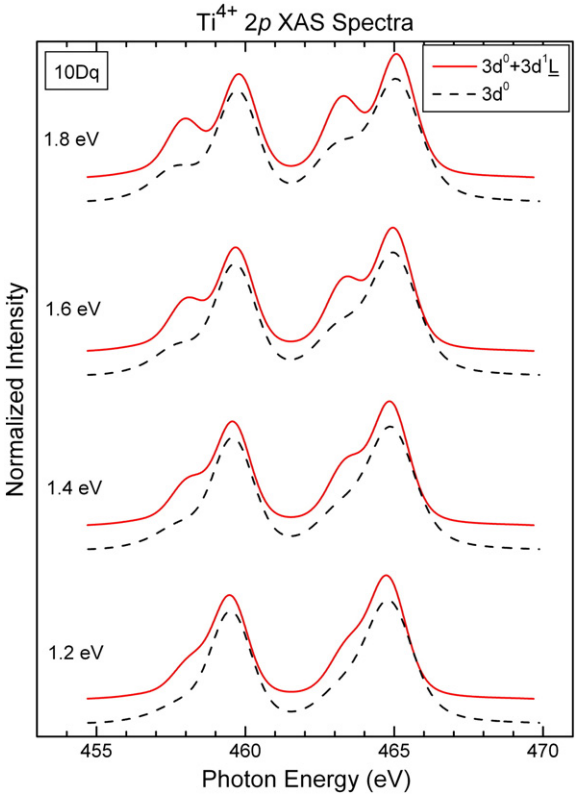

Fig. 3. Ti 2p XAS spectra for different crystal field (10 Dq) parameters calculated with the atomic multiplet method within the first $3d^0$ ionic approximation (dashed line), as well as including the interaction with the $3d^1\underline{L}$ configuration (solid line). The values of the crystal field (10 Dq) and Ti 3d–O 2p hybridization used in the calculation are listed in Table 1.

and Ti e_g states, whereas the peaks at 463.2 and 465.0 eV are due to transitions from the Ti $2p_{1/2}$ to Ti t_{2g} and Ti e_g states.

On the other hand, the Ti 2p XAS spectra for coverages below one equivalent TiO_2 monolayer grown on MgO, Al_2O_3 and SiO_2 show significant differences from those of bulk TiO_2, especially those grown on more covalent substrates, i.e. Al_2O_3 and SiO_2. The energy difference between the Ti t_{2g} and Ti e_g peaks decreases along the series. Further, the relative intensity of the Ti t_{2g} peak also decreases from the MgO to the SiO_2 substrates. First of all, we have to note that all the spectra for low coverages correspond to Ti^{4+} ions, as otherwise the spectra of other oxidation states would be broader and shifted in energy [38–40]. The differences in the spectra are attributed to changes in the crystal field and the Ti 3d–O 2p hybridization. In fact, Fig. 4 shows that the calculated atomic multiplet spectra are in very good agreement with the experimental results. The value of the crystal field parameter 10 Dq decreases from 1.8 eV for bulk TiO_2 to 1.2 eV for TiO_2/SiO_2, see Table 1. Further, the hybridization parameter pdσ is reduced from 2.1 eV for bulk TiO_2 to 1.5 eV for TiO_2/SiO_2, see Table 1. We have to note here that the values of the hybridization parameter correspond to the TiO_2 monolayer and not to the substrates. In fact, the increase of the covalent character of the substrates results in a decrease of the hybridization within the TiO_2 cluster, see below.

Gracia et al. reported that the Ti^{4+} ions were in tetrahedral symmetry in mixed SiO_2/TiO_2 oxides [41]. For a small amount of TiO_2 deposited on SiO_2 we expect less structural constrains than in a SiO_2/TiO_2 mixed oxide. We cannot completely rule out the presence of Ti^{4+} ions in tetrahedral coordination at the interface for the one monolayer films. In principle, this would also affect both the crystal field splitting and the effective Ti 3d–O 2p hybridization. In fact, this could explain the reduction of the covalence of the TiO_2 overlayer on MgO since the Ti–O–Mg bonds should be similar to the Ti–O–Ti bonds. Although the spectra for thicker films are consistent with the spectrum of our bulk TiO_2 reference sample, the spectrum of the TiO_2 monolayer on MgO does not show the splitting of the e_g peak as in bulk TiO_2 (see Fig. 4). This indicates that the bulk structure of TiO_2 has not been yet formed and suggests an octahedral coordination. Besides, it is known that TiO_2 can be epitaxialy grown on MgO [16] and our MgO substrate shows small faceted crystals (see Fig. 1).

The decrease of the crystal field splitting and Ti 3d–O 2p hybridization is assigned to changes in the electronic structure at the TiO_2/oxide interface. These changes were already attributed to the formation of cross-linking Ti–O–M (M = Mg, Al, and Si) bonds [11–13,20]. Quantum mechanical cluster calculations show that the O 2p levels appear at lower energies, giving rise to an increase of the band gap in the Ti–O–Ti, Ti–O–Mg, Ti–O–Al, and Ti–O–Si series [13,42]. This effect also reduces the covalent contribution to the bonding and the effective crystal field splitting [13].

Table 2
Ground state composition and Ti 3d electron count.

		TiO_2	TiO_2/MgO	TiO_2/Al_2O_3	TiO_2/SiO_2
Ground state composition (%)	$3d^0$	38.9	41.8	45.2	49.2
	$3d^1\underline{L}$	46.5	45.7	44.4	42.5
	$3d^2\underline{L}^2$	13.3	11.5	9.7	7.8
Ti 3d count		0.77	0.72	0.66	0.59

4.3. Cluster model calculations

Table 2 shows the contribution of the different configurations to the ground state of TiO_2, as well as of the TiO_2 thin films grown on the

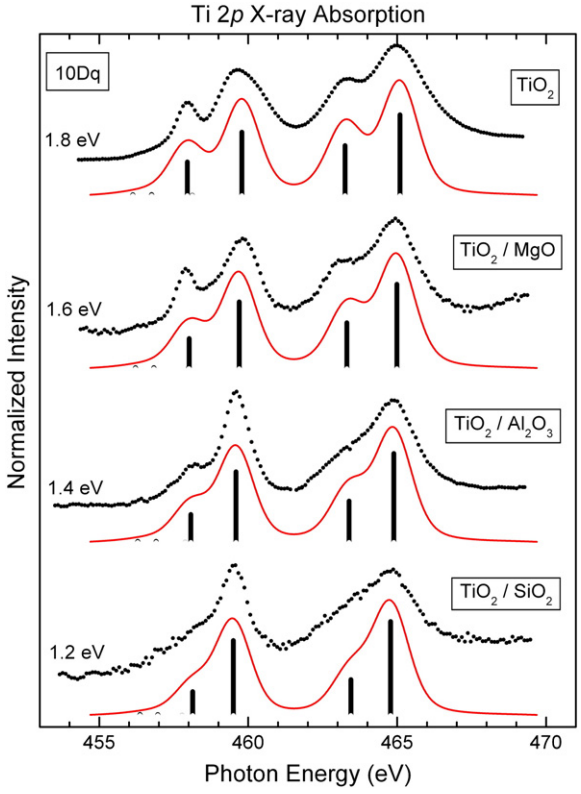

Fig. 4. Experimental (dots) and calculated (solid line) Ti 2p XAS spectra of the TiO_2 reference sample, as well as of the TiO_2 thin films grown on MgO, Al_2O_3, and SiO_2. The values of the crystal field (10 Dq) and Ti 3d–O 2p hybridization used in the calculation are listed in Table 1.

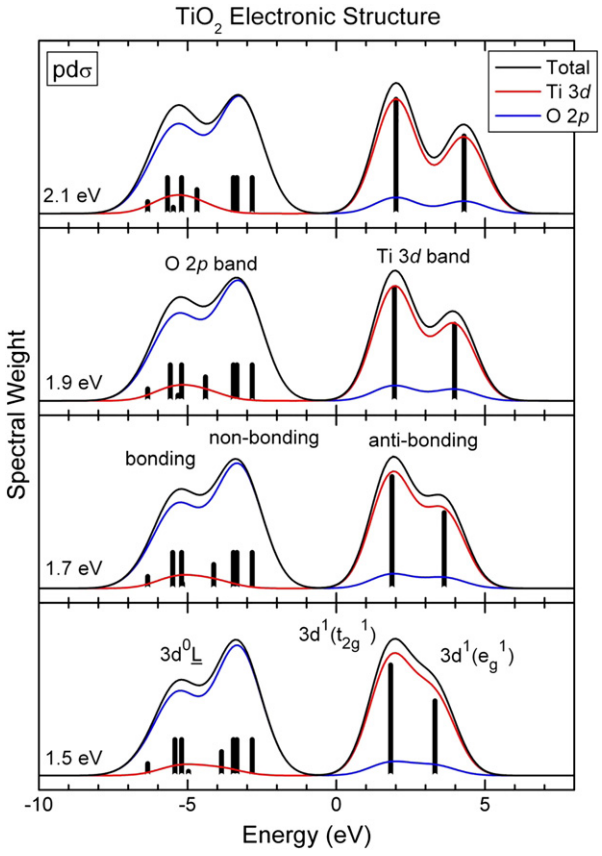

Fig. 5. Spectral weight calculated for a TiO_6 cluster in octahedral symmetry. The total spectral weight (black line) is projected into the partial O 2p (blue line) and partial Ti 3d (red line) contributions. The values of the crystal field (10 Dq) and Ti 3d–O 2p hybridization used in the calculation are listed in Table 1.

different oxide substrates. The reduction of the crystal field and hybridization parameters were obtained from the experimental Ti 2p XAS spectra. This reduction takes into account the effective influence of the substrates in the ground state of the thin films. The relative weight of the $3d^0$ configuration increases from the TiO_2/MgO to the TiO_2/SiO_2 interfaces. This indicates an increase of the ionic character of the thin films, which is also reflected by the reduction of the Ti 3d count. This trend is related to the formation of the Ti–O–M cross-linking bonds, as explained above.

Fig. 5 shows the calculated spectral weight of TiO_2 and TiO_2 thin films grown on the different oxides. The removal spectra are mostly dominated by the $3d^0 \rightarrow 3d^0\underline{L}$ transitions, whereas the addition spectra are mainly related to the $3d^0\underline{} \rightarrow 3d^1$ transitions. The discrete transitions were broadened with a Gaussian function to simulate the dispersion of the bands. The total spectral weight is projected into the partial Ti 3d and O 2p contributions. The valence band is mostly composed by the O 2p states, whereas the conduction band is mainly formed by the Ti 3d states. The bottom of the O 2p band presents mostly bonding character, whereas the top is mainly dominated by non-bonding states. The Ti 3d band presents mostly anti-bonding character, and is split by crystal field effects into the t_{2g} and e_g sub-bands.

The reduction of the crystal field and hybridization produces two main changes across the series: (i) the Ti 3d contribution to the valence band shifts to lower energies and (ii) the splitting between the Ti t_{2g} and the Ti e_g sub-bands diminishes. The first effect is mostly related with the reduction of the hybridization, whereas the later effect is mainly due to the decrease of the crystal field. This reduction is again expected to reproduce the experimental changes in the electronic structure of the different interfaces.

4.4. Valence band RPES spectra

The RPES spectra can be used to extract the Ti 3d contribution from the O 2p states in the valence band. This is achieved by the subtraction of the on-resonance and the off-resonance valence band spectra. Fig. 6 (top panel) shows the valence band spectrum of TiO_2 taken at $h\nu = 480$ eV (off-resonance). The total spectral weight is in agreement with the experimental result, since the Ti 3d and O 2p cross sections are similar at this energy [43]. Fig. 6 (bottom panel) shows the estimated Ti 3d contribution to the valence band of TiO_2, obtained from the subtraction of the spectrum taken at $h\nu = 458$ eV (on-resonance) and at $h\nu = 480$ eV (off-resonance). The calculated partial Ti 3d spectral weight is in good agreement with this experimental estimate.

Fig. 7 shows the Ti 3d contribution to the valence band of the TiO_2 thin films grown on MgO, Al_2O_3 and SiO_2. These contributions were obtained following the same procedure described above for the TiO_2 reference sample. The Ti 3d states shift by 0.8 eV towards lower energies as one goes from the MgO to the SiO_2 substrate. In addition, the width of the Ti 3d states also increases from 2.5 eV for MgO to 3.7 eV for SiO_2. The shift is attributed to the reduction of the crystal field and Ti 3d–O 2p interactions, which, as explained above, are due to the formation of the Ti–O–M bonds at the interface.

Fig. 7 also compares the calculated Ti 3d contribution to the valence band with the experimental results. The reduction of the crystal field (10 Dq) and hybridization (pdσ) parameters were obtained from the Ti 2p XAS spectra. The cluster model calculations reproduce both the energy shift and the broadening of the Ti 3d states. The energy shift is mainly related to the decrease of the Ti 3d–O 2p hybridization (pdσ), whereas the broadening results from the effect of the residual O 2p–O 2p interactions (ppσ).

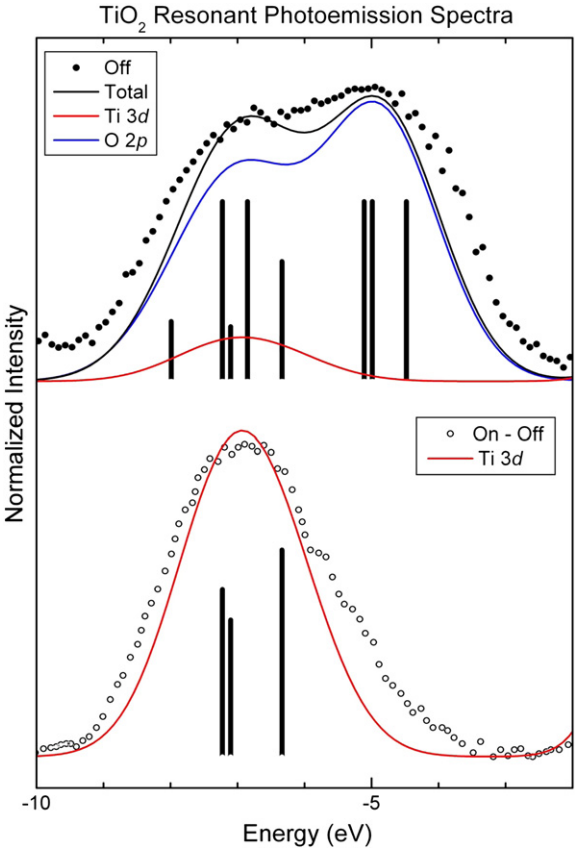

Fig. 6. (Top panel) Experimental (dots) valence band PES spectra of bulk TiO_2 taken at 480 eV (off-resonance) compared to total spectral weight (solid line) of the TiO_6 cluster. Partial Ti 3d and O 2p density of states are also indicated. (Bottom panel) Experimental Ti 3d states (dots) obtained by the on-off resonance RPES spectra of bulk TiO_2 compared to the partial Ti 3d contribution (solid line) of the TiO_6 cluster.

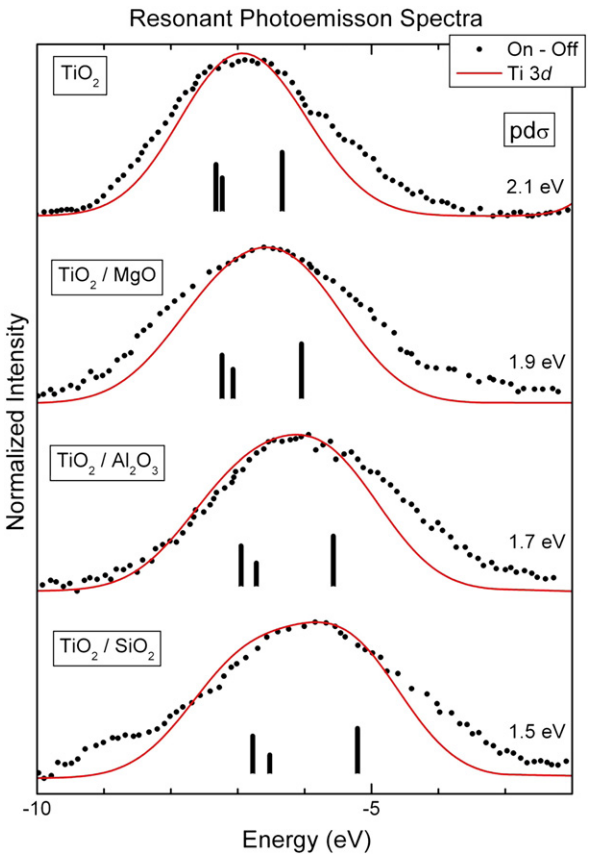

Fig. 7. Experimental (dots) and calculated (solid line) Ti 3d states of bulk TiO_2, as well as of the TiO_2 equivalent monolayers grown on MgO, Al_2O_3, and SiO_2. The values of the crystal field (10 Dq) and Ti 3d–O 2p hybridization used in the calculation are listed in Table 1.

These results show that the Ti–O–M bonds at the interface affects the electronic structure of TiO_2. In particular, the interface effect reduces the effective crystal field and hybridization of the TiO_2 thin films. The reduction increases systematically from the MgO to the SiO_2 substrate, as explained above. The changes in the electronic structure by the substrates would affect the physical properties of the TiO_2 thin films. These changes will be stronger for TiO_2/SiO_2 nanoparticles, where the surface-volume ratio would be significantly higher.

5. Conclusions

In summary, we studied the electronic structure of TiO_2 thin films grown on different oxide substrates. The effect of the support on the electronic structure of the TiO_2 was followed by Ti 2p XAS and RPES spectra. The Ti 2p XAS results evidence a significant reduction of the crystal field and the effective Ti 3d–O 2p hybridization. These reductions increase systematically along the $MgO–Al_2O_3–SiO_2$ series. Further, the Ti 3d states in the valence band, obtained from RPES, shift to lower energies along the series. This shift is mostly related with the reduction of the Ti 3d–O 2p hybridization mentioned above. These effects are attributed to the formation of cross-linking Ti–O–M (M = Mg, Al, and Si) bonds at the interface. In this picture, the O 2p states are also bonded to the M ions, affecting the strength of the effective Ti 3d–O 2p interactions. These findings not only provide important information on the study of oxide/oxide interfaces, but also open new perspectives in the study of modifications of ultra-thin-films grown on oxide substrates.

Acknowledgments

This work has been financially supported by the Spanish Ministerio de Ciencia e Innovación (MICINN) through contracts FUNCOAT-CSD2008-00023, MAT2007-66719-C03-03 and MAT2008-01497. The research leading to these results has received funding from the European Community's Seventh Framework Programme (FP7/2007–2013) under grant agreement no. 226716.

References

[1] G.H. Vurens, M. Salmerón, G.A. Somorjai, Prog. Surf. Sci. 32 (1990) 333.
[2] V.E. Henrich, Prog. Surf. Sci. 50 (1995) 77.
[3] V.E. Henrich, P.A. Cox, The Surface Science of Metal Oxides, University Press, Cambridge, 1994, Chapter 7.
[4] R.J. Lad, Surf. Rev. Lett. 2 (1995) 109.
[5] A.R. González-Elipe, F. Yubero, in: H.S. Nalwa (Ed.), Handbook of Surfaces and Interfaces of Materials, Academic Press, San Diego, 2001, Chapter 4.
[6] A. Barranco, F. Yubero, J.P. Espinós, A.R. González-Elipe, Surf. Interface Anal. 31 (2001) 761.
[7] M. Reddy, B.M. Khan, A. Catal. Rev. 47 (2005) 257.
[8] M. Bibes, A. Barthélémy, IEEE Trans. Electron Devices 54 (2007) 1003.
[9] J.W. Fergus, Sens. Actuators B 123 (2007) 1169.
[10] C.H. Ahn, A. Bhattacharya, M. Di Ventra, J.N. Eckstein, C.D. Frisbie, M.E. Gershenson, A.M. Goldman, I.H. Inoue, J. Mannhart, A.J. Millis, A.F. Morpurgo, N. Douglas, Rev. Mod. Phys. 78 (2006) 1185.
[11] G. Lassaleta, A. Fernández, J.P. Espinós, A.R. González-Elipe, J. Phys. Chem. 99 (1995) 1484.
[12] J.P. Espinós, G. Lassaleta, A. Caballero, A. Fernández, A.R. González-Elipe, A. Stampfl, C. Morant, J.M. Sanz, Langmuir 14 (1998) 4908.
[13] J.A. Mejías, V.M. Jiménez, G. Lassaletta, A. Fernández, J.P. Espinós, A.R. González-Elipe, J. Phys. Chem. 100 (1996) 16255.
[14] H.L.M. Chang, H. You, Y. Gao, J. Guo, C.M. Foster, R.P. Chiarello, T.J. Zhang, D.J. Lam, J. Mater. Res. 7 (1992) 2495.
[15] H.L.M. Chang, T.J. Zhang, H. Zhang, J. Guo, H.K. Kim, D.J. Lam, J. Mater. Res. 8 (1993) 2634.
[16] S. Watanabe, K. Katsura, H. Nozoye, Jpn. J. Appl. Phys. 38 (1999) L62.
[17] J.C. Fuggle, J. Inglesfield, Unoccupied Electronic States, Springer, Berlin, 1992.
[18] J.G. Chen, Surf. Sci. Rep. 30 (1997) 1.
[19] F.J. Himpsel, U.O. Karlsson, A.B. McLean, L. Terminello, F.M.F. de Groot, M. Abbate, J.C. Fuggle, J.A. Yarmoff, B.T. Thole, G.A. Sawatzky, Phys. Rev. B 43 (1991) 6899.
[20] L. Soriano, G.G. Fuentes, C. Quirós, J.F. Trigo, J.M. Sanz, P.R. Bressler, A.R. González-Elipe, Langmuir 16 (2000) 7066.
[21] M. Sánchez-Agudo, L. Soriano, C. Quirós, J. Avila, J.M. Sanz, Surf. Sci. 482 (2001) 470.
[22] L. Soriano, A. Gutiérrez, I. Preda, S. Palacín, J.M. Sanz, M. Abbate, J.F. Trigo, A. Vollmer, P.R. Bressler, Phys. Rev. B 74 (2006) 193402.
[23] L.C. Davis, J. Appl. Phys. 59 (1986) R25.
[24] S. Bourgeois, B. Domenichini, Z. Li, P.J. Møller, Appl. Surf. Sci. 244 (2005) 399.
[25] Z.M. Zhang, S.P. Jeng, V.E. Henrich, Phys. Rev. B 43 (1991) 12004.
[26] R. Heise, R. Courths, S. Witzel, Solid State Commun. 84 (1992) 599.
[27] K.C. Prince, V.R. Dhanak, P. Finetti, J.F. Walsh, R. Davis, C.A. Muryn, H.S. Dhariwal, G. Thornton, G. Van der Laan, Phys. Rev. B 55 (1997) 9520.
[28] M. Sánchez-Agudo, L. Soriano, J.F. Trigo, C. Quirós, G.G. Fuentes, C. Morant, E. Elizalde, J.M. Sanz, Surf. Interface Anal. 34 (2002) 244.
[29] M. Sánchez-Agudo, L. Soriano, C. Quirós, M. Abbate, L. Roca, J. Avila, J.M. Sanz, Langmuir 17 (2001) 7339.
[30] M. Sánchez-Agudo, L. Soriano, R. Fernández-Jiménez, A. Gutiérrez, M. Abbate, S. Wiklund, J.M. Sanz, Surf. Sci. 566 (2004) 515.
[31] I. Preda, A. Gutiérrez, M. Abbate, F. Yubero, J. Méndez, L. Alvarez, L. Soriano, Phys. Rev. B 77 (2008) 075411.
[32] BESSY User's Handbook, BESSY, Berlin, 1998.
[33] R. Brydson, H. Sauer, W. Engel, J.M. Thomas, E. Zeitler, N. Kosugi, H.J. Kuroda, J. Phys. Condens. Matter 1 (1989) 797.
[34] I. Horcas, R. Fernández, J.M. Gómez-Rodríguez, J. Colchero, J. Gómez-Herrero, A.M. Baró, Rev. Sci. Instrum. 78 (2007) 013705.
[35] A.E. Bocquet, T. Mizokawa, K. Morikawa, A. Fujimori, S.R. Barman, K. Maiti, D.D. Sarma, Y. Tokura, M. Onoda, Phys. Rev. B 53 (1996) 1161.
[36] M. Grioni, M.T. Czyzyk, F.M.F. de Groot, J.C. Fuggle, B.E. Watts, Phys. Rev. B 39 (1989) 4886.
[37] F.M.F. de Groot, J.C. Fuggle, B.T. Thole, G.A. Sawatzky, Phys. Rev. B 41 (1990) 928, 42 (1990) 5459.
[38] V.S. Lusvardi, M.A. Barteau, J.G. Chen, J. Eng Jr., B. Frühberger, A. Teplyakov, Surf. Sci. 397 (1998) 237.
[39] L. Soriano, M. Abbate, F.M.F. de Groot, D. Alders, J.C. Fuggle, S. Hofmann, H. Petersen, W. Braun, Surf. Interface Anal. 20 (1993) 21.
[40] L. Soriano, M. Abbate, J. Vogel, J.C. Fuggle, A. Fernández, A.R. González-Elipe, M. Sacchi, J.M. Sanz, Surf. Sci. 290 (1993) 427.
[41] F. Gracia, F. Yubero, J.P. Holgado, J.P. Espinós, A.R. González-Elipe, T. Girardeau, Thin Solid Films 500 (2006) 19.
[42] F.J. Ferrer, F. Yubero, J.A. Mejías, F.J. García-Lopez, A.R. González-Elipe, J. Appl. Phys. 102 (2007) 084112.
[43] J.-J. Yeh, I. Lindau, At. Data Nucl. Data Tables 32 (1985) 1.